Elastic analysis of interfacial stress concentrations in CFRP-RC hybrid beams: Effect of creep and shrinkage

Rabahi Abderezak [1,2], Tahar Hassaine Daouadji [*1,2], Boussad Abbes [3],
Benferhat Rabia [1,2], Adim Belkacem [2,4] and Fazilay Abbes [3]

[1] *Département de génie civil , Université Ibn Khaldoun Tiaret, BP 78 Zaaroura, Tiaret, Algérie*
[2] *Laboratoire de Géomatique et Développement Durable, Université de Tiaret, Algérie*
[3] *Laboratoire GRESPI—Campus du Moulin de la Housse, Reims Cedex 2, France*
[4] *Département des sciences et technologies, Centre Universitaire Tissemsilt, Algérie*

Abstract. A simple closed-form solution to calculate the interfacial shear and normal stresses of retrofitted concrete beam strengthened with thin composite plate under mechanical loads including the creep and shrinkage effect has been presented in this paper. In such plated beams, tensile forces develop in the bonded plate, and these have to be transferred to the original beam via interfacial shear and normal stresses. Consequently, debonding failure may occur at the plate ends due to a combination of high shear and normal interfacial stresses. These stresses between a beam and a soffit plate, within the linear elastic range, have been addressed by numerous analytical investigations. Surprisingly, none of these investigations has examined interfacial stresses while taking the creep and shrinkage effect into account. In the present theoretical analysis for the interfacial stresses between reinforced concrete beam and a thin composite plate bonded to its soffit, the influence of creep and shrinkage effect relative to the time of the casting, and the time of the loading of the beams is taken into account. Numerical results from the present analysis are presented both to demonstrate the advantages of the present solution over existing ones and to illustrate the main characteristics of interfacial stress distributions.

Keywords: interfacial stresses; strengthening; creep; shrinkage; concrete beam; FRP composite

1. Introduction

Advanced composite materials, e.g., fiber-reinforced polymers (FRP), have found new applications in the rehabilitation of reinforced concrete structures. Compared with the traditional materials, composite materials have some unique features, namely, high strength and stiffness to weight ratio, attractive corrosion resistance and ease of handling and application. The rehabilitation or strengthening of reinforced concrete structures is an important problem in civil engineering. In the last few years, FRP composites are being used in the construction industry in the form of laminates and pultruded plates for strengthening of existing structures Meier (1995). With their excellent properties such as high tensile strength, long-term durability, corrosion/fire resistance and low weight, FRPs have almost completely replaced steel plates as externally epoxy-

---

∗Corresponding author, Ph.D., Professor, E-mail: daouadjitahar@gmail.com

bonded reinforcement for concrete. An important failure mode for such members is the debonding of the FRP plate from the member because of high interfacial stresses near the plate ends. Accurate predictions of the interfacial stresses are thus important for designing against debonding failures. Several closed-form solutions have been developed in the past decade for the interfacial stresses in beams bonded with a steel or FRP plate (Tounsi *et al*. 2009 and Hassaine Daouadji *et al*. 2008). All these solutions are for linear elastic materials and employ the same key assumption that the adhesive is subject to normal and shear stresses that are constant across the thickness of the adhesive layer. It is this key assumption that enables relatively simple closed-form solutions to be obtained. In the existing solutions, two different approaches have been employed. Roberts and Hajikazemi (1989) used a staged analysis approach, while (Vilnay 1988, Taljsten 1997, Tounsi *et al*. 2009, Hassaine Daouadji 2013, Smith and Teng 2001, Benyoucef *et al*. 2014, Bouakaz *et al*. 2014, Guenaneche and Tounsi 2014, Mahi *et al*. 2014, Touati *et al*. 2015, Zidani *et al*. 2015 and Krour *et al*. 2013) considered directly deformation compatibility conditions. Rabinovitch and Frostig (2001) have presented a higher order analysis in which the adhesive layer was treated as an elastic medium with negligible longitudinal stiffness. This leads to uniform stresses and linearly varying normal stresses through the thickness of the adhesive layer. The significance of their solution is that it is the first solution that satisfies the stress-free boundary condition at the ends of the adhesive layer. Using the same approach, they investigated the effects of an uneven adhesive layer and material non linearity. They also evaluated the energy release rate to predict debonding failure Rabinovich and Frostig (2001). Shen *et al*. (2001), Yang *et al*. (2003) and Ameur *et al*. (2009) proposed an alternative analytical complementary energy approach, which resulted in closed-form expressions.

Interfacial stress studies accounting for the influence of adherend shear deformation are scarce. However, it is reasonable to assume that the shear stresses, which develop in the adhesive, are continuous across the adhesive–adherend interface. In addition, equilibrium requires the shear stress be zero at the free surface. The importance of including the shear-lag effect of the adherends was shown by several authors. Tounsi (2006) has extended this theory to study concrete beams strengthened by FRP plates. The basic assumption in these two studies is a linear distribution of shear stress across the thickness of the adherends. However, it is well known that, in beam theory, this distribution is parabolic through the depth of beam. The objective of the present investigation is to improve the method developed by Tounsi (2006) by assuming a parabolic shear stress across the depth of both FRP plate and RC beams and the effect of creep and shrinkage. In view of this, it is desirable that a solution methodology be developed where the effect of adherend shear deformations can be included in a better manner so that the accuracy of Tounsi's solution can be properly assessed. With this in mind, the objectives of this paper are first to present an improvement to Tounsi's solution to obtain a new closed-form solution which accounts for the parabolic adherend shear deformation effect in both the beam and bonded plate and second to compare quantitatively its solution against the new one developed in this paper by numerical illustrations. Numerical examples and a parametric study are presented to illustrate the governing parameters that control the creep and shrinkage effect on adhesive stress concentrations at the edge of the FRP strip. Finally, the adopted improved model describes better the actual response of the FRP- RC hybrid beams and permits the evaluation of the adhesive stresses, the knowledge of which is very important in the design of such structures. It is believed that the present results will be of interest to civil and structural engineers and researchers.

The majority of the studies mentioned have focused on the short-term response characteristics of concrete beams strengthened with a thin hygrothermal aged composite plate (Ameur *et al*. 2009

and Amara *et al*. 2005). In recent applications, the authors aim at developing a fundamental understanding of the time-dependent (creep and shrinkage) behavior of composite/concrete interface of RC beams strengthened with composite plates.

We can also mention, in addition to the composite fiber matrix materials, another alternative can be proposed to strengthen the structures that will be addressed in our future research, it is therefore the use of functionally graded materials (FGM) (Hebali *et al*. 2014, Draiche 2016, Hamidi *et al*. 2015 and Zidi *et al*. 2014) that in order to improve and ensure the material continuity through the thickness of the reinforcing plate, aiming as a parameter in the mechanical characteristics of FGM, all by passing laws adequately mixes to better meet industrial requirements and the environmental condition.

2. Theoretical analysis and solutions procedure of the present method

A differential section dx, can be cut out from the FRP reinforced concrete beam (Fig. 1), as shown in Fig. 2. The composite beam is made from three materials: reinforced concrete, adhesive and composite reinforcement. In the present analysis, linear elastic behaviour is regarded to be for all materials; the adhesive is assumed to play a role only in transferring the stresses from the concrete to the FRP reinforcement and the stresses in the adhesive layer do not change through the direction of the thickness.

2.1 Basic equation of elasticity

The strain $\varepsilon_b(x)$ in the concrete beam near adhesive interface can be expressed as

$$\varepsilon_b(x) = \frac{du_b(x)}{dx} = \frac{e\, M_b(x)}{E_b\, I_b} - \frac{N_b(x)}{E_b I_b} + \alpha\, T_b \tag{1}$$

where $u_b(x)$ means horizontal displacement of the RC beam near interface, $M_b(x)$ stands for bending moments applied in the concrete, I_b is the second moment area, e is distance from the neutral axis to the bottom of RC beam, N_b is the axial force applied in the concrete beam, A_b the cross-sectional area, the temperature T_b is defined in Eq. (9); $E_b = E_b(t)$ is the time dependent tangent modulus of elasticity of the concrete beam given as

$$E_b(t) = \frac{E_{bl}}{1 + \chi\varphi(t, tb)} \tag{2}$$

Where E_{bl} is the tangent modulus of elasticity of the beam at time t_{bl}; χ is an aging coefficient depending on strain development with time; and $t_b = t_{bl} - t_{bc}$ (t_{bc} is time of casting of beams and t_{bl} time at initial loading of beams); $\varphi(t, t_b)$ is the creep coefficient related to the elastic deformation at t_b days, which is defined as Eurocode 2 Editorial Group (1991)

$$\varphi(t, t_b) = \phi_{RH}\,\beta(f_{cm})\beta(t_b)\beta(t - t_b) \tag{3}$$

Where ϕ_{RH}, $\beta(f_{cm})$, and $\beta(t_b)$ are factors depending on the relative humidity, the concrete strength, and the concrete age loading, respectively, which are defined as
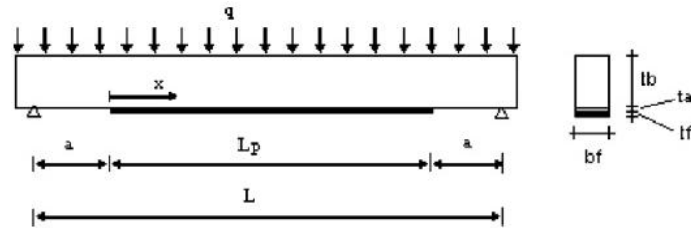
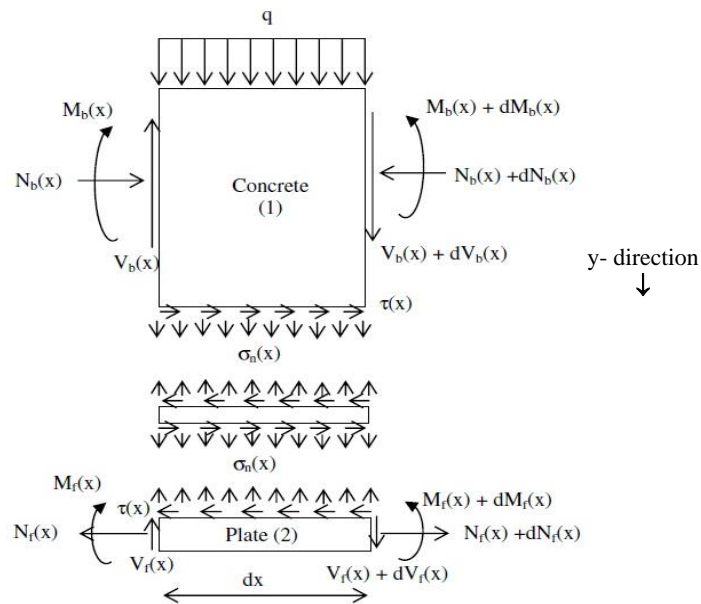Fig. 1 Simply supported beam strengthened with bonded FRP plate

Fig. 2 Forces in infinitesimal element of a soffit-plated beam

$$\phi_{RH} = 1 + \frac{(1 - RH/100)}{(0.10^3 \sqrt{h_0})} \tag{4}$$

$$\beta(f_{cm}) = \frac{16.8}{\sqrt{f_{cm}}} \tag{5}$$

$$\beta(t_p) = \frac{1}{(0.1 + t_p^{0.20})} \tag{6}$$

where RH is the relative humidity of the ambient environment in %, $h_0 = 2A_b / P_b$ is the notional size of the beam in mm; A_b is the area of the beam cross-section; P_b is the beam perimeter in contact with the atmosphere and f_{cm} is the mean compressive strength of concrete in N/mm^2 at the age 28 days. Moreover, $\beta_{cp}(t - t_p)$ in Eq. (3) is a coefficient for the development of creep with time, which is estimated from

$$\beta_{cp}\left(t-t_p\right)=\left[\frac{\left(t-t_p\right)}{\beta_H+t-t_p}\right]^{0.30} \tag{7}$$

Where β_H is a coefficient depending on the relative humidity *RH*, given as

$$\beta_H=1.5\left[1+\left(0.012RH\right)^{0.18}\right]\,h_0+250\leq1500 \tag{8}$$

Assuming that creep and shrinkage are independent, the temperature T_b in Eq. (1) is given as (Eurocode 2 Editorial Group)

$$T_b=\frac{\varepsilon_{sb}\left(t-t_{bc}\right)}{\alpha} \tag{9}$$

Where α is a linear coefficient of thermal expansion and $\varepsilon_{sb}(t-t_{bc})$ the shrinkage strain calculated from

$$\varepsilon_{sb}\left(t-t_{bc}\right)=\varepsilon_{sb}\left(f_{cm}\right)\beta_{RH}\,\beta_{sb}\left(t-t_{bc}\right) \tag{10}$$

Where $\varepsilon_{sb}(f_{cm})$ and β_{RH} are factors depending on the concrete strength and the relative humidity, respectively, which are defined as

$$\varepsilon_{sb}\left(f_{cm}\right)=\left[160+\beta_{sc}\left(90-f_{cm}\right)\right]10^{-6} \tag{11}$$

$$\beta_{RH}=\begin{cases}-1.55\left(1-\left(\dfrac{RH}{100}\right)^3\right), & pour\quad40\ \%\ \leq\ RH\ \leq99\ \% \\[3mm] +0.25\left(1-\left(\dfrac{RH}{100}\right)^3\right); & pour\quad RH\ \geq\ 99\ \%\end{cases} \qquad \begin{array}{l}\text{(Stored in air)}\\ \text{(Immersed in water)}\end{array} \tag{12}$$

Where β_{sc} is a coefficient depending on type of cement. Moreover, $\beta_{sb}(t-t_{bc})$ in Eq. (10) is a coefficient for the development of shrinkage with time, which is estimated from

$$\beta_{sb}\left(t-t_{bc}\right)=\left[\frac{t-t_{bc}}{0035{h_0}^2+t-t_{bc}}\right]^{0.5} \tag{13}$$

Now, to estimate the strain $e_f(x)$ in the external FRP reinforcement near adhesive interface we have used the laminate theory. Furthermore, it is assumed that the ply arrangement of the plate is symmetrical

$$\varepsilon_f\left(x\right)=\frac{du_f}{dx}=-D_{11}'\frac{t_f}{2b_f}M_f\left(x\right)+A_{11}'\frac{N_f\left(x\right)}{b_f} \tag{14}$$

where $\varepsilon_f(x)$ means horizontal displacement of the external FRP reinforcement near interface; $M_f(x)$ represents the bending moment applied in the external FRP reinforcement, N_f stands for the axial force applied in the external FRP reinforcement; b_f is the width of the plate; t_f is thickness of the external reinforcement; $[A'] = [A^{-1}]$ is the inverse of the extensional matrix $[A']$; and $[D'] = [D^{-1}]$ is the inverse of the flexural matrix. $[D']$

By adopting the equilibrium conditions of the concrete, we have

$$x\text{-direction:} \qquad \frac{dN_b(x)}{dx} = b_f \tau(x) \qquad\qquad (15)$$

Where $\tau(x)$ is shear stress in the adhesive layer.

$$y\text{-direction:} \qquad \frac{dV_b(x)}{dx} = -[\sigma_n(x)b_f + q] \qquad\qquad (16)$$

Where $V_b(x)$ means the shear force applied in the concrete; $\sigma_n(x)$ means the normal stress in the adhesive layer and q is the uniformly distributed load.

$$\text{Moment equilibrium:} \qquad \frac{dM_b(x)}{dx} = V_b(x) - \tau(x)b_f e \qquad\qquad (17)$$

The equilibrium of the external FRP reinforcement along the *x*, *y*-direction and moment equilibrium can also be written as

$$\frac{dN_f(x)}{dx} = b_f \tau(x) \qquad\qquad (18)$$

$$\frac{dV_b(x)}{dx} = b_f \sigma(x) \qquad\qquad (19)$$

$$\frac{dM_f(x)}{dx} = V_f(x) - \tau(x)b_f \frac{t_f}{2} \qquad\qquad (20)$$

Where $V_f(x)$ means the shear force applied in the external FRP reinforcement.

2.2 Shear stress distribution along the FRP plate – concrete interface

The shear stress in the adhesive can be expressed as follows

$$\tau(x) = \frac{G_a}{t_a} \Delta u(x) = \frac{G_a}{t_a}[u_f(x) - u_b(x)] \qquad\qquad (21)$$

Where $\Delta u(x)$ is relative horizontal displacement at the adhesive interface, G_a is the shear modulus in the adhesive and t_a is the thickness of the adhesive.
By differentiating Eq. (21) and by using Eqs. (1) and (14)

$$\frac{d\tau(x)}{dx} = \frac{G_a}{t_a}\left[A_{11}' \frac{N_f(x)}{b_f} - D_{11}' \frac{t_f}{2b_f} M_f(x) - \frac{e}{E_b I_b} M_b(x) + \frac{N_b(x)}{E_b A_b} - \alpha\, T_b \right] \qquad\qquad (22)$$

Assuming equal curvature in the beam and the FRP plate, the relationship between the moments in the two adherends can be expressed as

$$M_b(x) = RM_f(x) \tag{23}$$

With: $$R = \frac{E_b I_b D_{11}'}{b_f} \tag{24}$$

Moment equilibrium of the differential segment of the plated beam in Fig. 2 gives

$$M_T(x) = M_b(x) + M_f(x) + N(x)\left[e + \frac{t_f}{2} + t_a\right] \tag{25}$$

Where $M_{T(x)}$ is the total applied moment and from Eqs. (15) and (18), the axial forces are given as

$$N_b(x) = N_f(x) = N(x) = b_f \int_0^x \tau(x)\,dx \tag{26}$$

The bending moment in each adherend, expressed as a function of the total applied moment and the interfacial shear stress, is given as

$$M_b(x) = \frac{R}{R+1}\left[M_T(x) - b_f \int_0^x \tau(x)\left(e + \frac{t_f}{2} + t_a\right)dx\right] \tag{27}$$

And

$$M_f(x) = \frac{1}{R+1}\left[M_T(x) - b_f \int_0^x \tau(x)\left(e + \frac{t_f}{2} + t_a\right)dx\right] \tag{28}$$

The first derivative of the bending moment in each adherend gives

$$\frac{dM_b(x)}{dx} = \frac{R}{R+1}\left[V_T(x) - b_f \tau(x)\left(e + \frac{t_f}{2} + t_a\right)\right] \tag{29}$$

And

$$\frac{dM_f(x)}{dx} = \frac{1}{R+1}\left[V_T(x) - b_f \tau(x)\left(e + \frac{t_f}{2} + t_a\right)\right] \tag{30}$$

By differentiating Eq. (22), we obtain

$$\frac{d^2\tau(x)}{dx^2} = \frac{G_a}{t_a}\left(\frac{-t_f}{2b_f}D_{11}'\frac{dM_f}{dx} + \frac{A_{11}'}{b_f}\frac{dN_f(x)}{dx} - \frac{e}{E_b I_b}\frac{dM_b(x)}{dx} + \frac{1}{E_b A_b}\frac{dN_b(x)}{dx}\right) \tag{31}$$

Substitution of the shear forces (Eqs. (29) and (30)) and axial forces (Eq. (26)) in both adherends into Eq. (31) gives the following governing differential equation for the interfacial shear stress

$$\frac{d^2\tau(x)}{dx^2} - \frac{G_a}{t_a}\left[A_{11} + \frac{b_f}{E_b A_b} + \frac{\left(e + \frac{t_f}{2}\right)\left(e + \frac{t_f}{2} + t_a\right)}{E_b I_b D_{11}' + b_f}b_f D_{11}'\right]\tau(x) + \frac{G_a}{t_a}\left(\frac{e + \frac{t_f}{2}}{E_b I_b D_{11}' + b_f}D_{11}'\right)V_T(x) = 0 \quad (32)$$

For simplicity, the general solutions presented below are limited to loading which is either concentrated or uniformly distributed over part or the whole span of the beam, or both. For such loading, $d^2V_T(x)/dx^2 = 0$, and the general solution to Eq. (32) is given by

$$\tau(x) = B_1 \cosh(\lambda x) + B_2 \sinh(\lambda x) + m_1 V_T(x) \quad (33)$$

Where

$$\lambda^2 = \frac{G_a}{t_a}\left(A_{11}' + \frac{b_f}{E_b A_b} + \frac{\left(e + \frac{t_f}{2}\right)\left(e + \frac{t_2}{2} + t_a\right)}{E_b I_b D_{11}' + b_f}b_f D_{11}'\right) \quad (34)$$

And

$$m_1 = \frac{G_a}{t_a \lambda^2}\left(\frac{e + \frac{t_2}{2}}{E_b I_b D_{11}' + b_f}D_{11}'\right) \quad (35)$$

B_1 and B_2 are constant coefficients determined from the boundary conditions.

2.3 Normal stress distribution along the FRP plate - concrete interface

The normal stress in the adhesive can be expressed as follows

$$\sigma_n(x) = K_n \Delta w(x) = K_n \left[w_f(x) - w_b(x)\right] \quad (36)$$

Where K_n is normal stiffness of the adhesive per unit length and can be deduced as

$$K_n = \frac{\sigma_n(x)}{\Delta w(x)} = \frac{\sigma_n(x)}{\Delta w(x)/t_a}\left(\frac{1}{t_a}\right) = \frac{E_a}{t_a} \quad (37)$$

Where $w_b(x)$ and $w_f(x)$ are the vertical displacements of RC beam and FRP plate, respectively. Differentiating Eq. (36) twice results in

$$\frac{d^2\sigma_n(x)}{dx^2} = K_n \left[\frac{d^2w_f(x)}{dx^2} - \frac{d^2w_b(x)}{dx^2}\right] \quad (38)$$

Considering the moment–curvature relationships for the beam to be strengthened and the

external reinforcement, respectively

$$\frac{d^2 w_b(x)}{dx^2} = -\frac{M_b(x)}{E_b I_b} \quad , \qquad \frac{d^2 w_2(x)}{dx^2} = -\frac{D_{11} M_f(x)'}{b_f} \tag{39}$$

Based on the equilibrium Eqs. (15)-(20), the governing differential equations for the deflection of adherends 1 and 2, expressed in terms of the interfacial shear and normal stresses, are given as follows

Adherend 1: $\qquad \dfrac{d^4 w_b(x)}{dx^4} = \dfrac{1}{E_b I_b} b_f \sigma_n(x) + \dfrac{e}{E_b I_b} b_f \dfrac{d\tau(x)}{dx} + \dfrac{q}{E_b I_b}$ (40)

Adherend 2: $\qquad \dfrac{d^4 w_f(x)}{dx^4} = -D_{11}' \sigma(x) + D_{11}' \dfrac{t_f}{2} \dfrac{d\tau(x)}{dx}$ (41)

Substitution of Eqs. (40) and (41) into the fourth derivation of the interfacial normal stress obtainable from Eq. (36) gives the following governing differential equation for the interfacial normal stress

$$\frac{d^4 \sigma_n(x)}{dx^4} + K_n \left(D_{11}' + \frac{b_f}{E_b I_b} \right) \sigma_n(x) - K_n \left(D_{11}' \frac{t_f}{2} - \frac{e b_f}{E_b I_b} \right) \frac{d\tau(x)}{dx} + \frac{q K_n}{E_b I_b} = 0 \tag{42}$$

The general solution to this fourth-order differential equation is

$$\sigma_n(x) = e^{-\beta x} \left[C_1 \cos (\beta x) + C_2 \sin (\beta x) \right] + e^{\beta x} \left[C_3 \cos (\beta x) + C_4 \sin (\beta x) \right] - n_1 \frac{d\tau(x)}{dx} - n_2 q \tag{43}$$

For large values of x it is assumed that the normal stress approaches zero, and as a result $C_3 = C_4 = 0$. The general solution therefore becomes

$$\sigma_n(x) = e^{-\beta x} \left[C_1 \cos (\beta x) + C_2 \sin (\beta x) \right] - n_1 \frac{d\tau(x)}{dx} - n_2 q \tag{44}$$

Where

$$\beta = \sqrt[4]{\frac{K_n}{4} \left(\frac{b_f}{E_b I_b} + D_{11}' \right)} \tag{45}$$

$$n_1 = \left(\frac{e b_f - D_{11}' E_b I_b \dfrac{t_f}{2}}{D_{11}' E_b I_b + b_f} \right) \tag{46}$$

$$n_2 = \frac{1}{D_{11}' E_b I_b + b_f} \tag{47}$$

C_1 and C_2 are constant coefficients determined from the boundary conditions.

2.4 Application of boundary conditions

The same loads cases used by Smith and Teng (2001) are considered in the present method. A simply supported beam is investigated which is subjected to a uniformly distributed load and an arbitrarily positioned single point load as shown in Fig. 3. This section derives the expressions of the interfacial shear and normal stresses for each load case by applying suitable boundary conditions.

Interfacial shear stress for a uniformly distributed load:

As is described by Smith and Teng (2001) the interfacial shear stress for this load case at any point is written as. The constants of integration need to be determined by applying suitable boundary conditions. The first boundary condition is applied at the bending moment at $x = 0$. Here, the moment at the plate end

$M_f(0)$ and the axial force of either the concrete beam or FRP plate $[N_b(0) = N_f(0)]$ are zero. As a result, the moment in the section at the plate curtailment is resisted by the beam alone and can be expressed as

$$M_b(0) = M_t(0) = \frac{qa}{2}(L - a) \tag{48}$$

Applying the above boundary condition in Eq. (22)

$$\frac{d\tau(x=0)}{dx} = -m_2 M_T(0); \qquad m_2 = \frac{G_a}{t_a}\left(\frac{e}{E_b I_b} + \frac{\alpha T_b}{M_T(0)}\right) \tag{49}$$
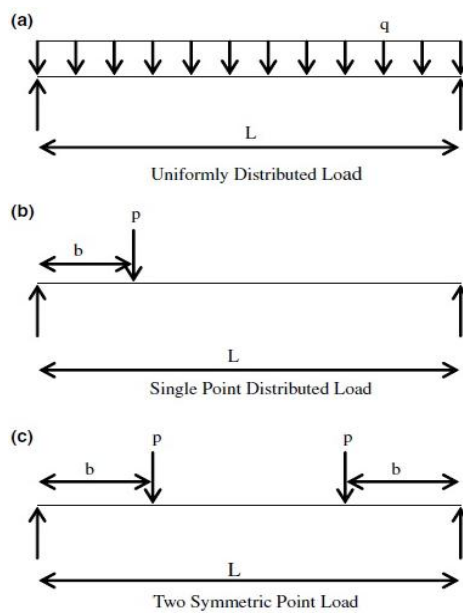

Fig. 3 Load cases

By substituting Eq. (33) into (49), B_2 can be determined as

$$B_2 = -\frac{q\,a\,m_2}{2\lambda}(L-a) + \frac{m_1}{\lambda}q \qquad (50)$$

The second boundary condition requires zero interfacial shear stress at mid-span due to symmetry of the applied load. B_1 can therefore be determined as

$$B_1 = \frac{a\,q\,m_2}{2\lambda}(L-a)\tanh\left(\frac{\lambda L_P}{2}\right) - \frac{q\,m_1}{\lambda}\tanh\left(\frac{\lambda L_p}{2}\right) \qquad (51)$$

For practical cases $\frac{\lambda L_\sigma}{2} > 10$ and as a result $\tanh\left(\frac{\lambda L_\sigma}{2}\right) \approx 1$. So the expression for B_1 can be simplified to

$$B_1 = \frac{a\,q\,m_2}{2\lambda}(L-a) - \frac{q\,m_1}{\lambda} = -B_2 \qquad (52)$$

Substitution of B_1 and B_2 into Eq. (33) gives an expression for the interfacial shear stress at any point

$$\tau(x) = \left[\frac{m_2 a}{2}(L-a) - m_1\right]\frac{qe^{-\lambda x}}{\lambda} + m_1 q\left(\frac{L}{2} - a - x\right) \qquad 0 \le x \le L_P \qquad (53)$$

$$m_2 = K_1\left(\frac{e}{E_1 I_1} + \frac{\alpha T_b}{M_T(0)}\right) \qquad (54)$$

where q is the uniformly distributed load and x, a, L and Lp are defined in Fig. 1. Contrary, to the method presented by Smith and Teng (2001), the expression of m_2 in the present method which take into account the shear deformations of adherends become:

Interfacial shear stress for a single point load
The general solution for the interfacial shear stress for this load case is

$$a < b: \qquad \tau(x) = \begin{cases} \dfrac{m_2}{\lambda}Pa\left(1 - \dfrac{b}{L}\right)e^{-\lambda x}\dfrac{q}{\lambda} + m_1 P\left(1 - \dfrac{b}{L}\right) - m_1 P\cosh(\lambda x)e^{-k} & 0 \le x \le (b\text{-}a) \\[3mm] \dfrac{m_2}{\lambda}Pa\left(1 - \dfrac{b}{L}\right)e^{-\lambda x}\dfrac{q}{\lambda} - m_1\dfrac{Pb}{L} + m_1 P\sinh(k)e^{-\lambda x} & (b\text{-}a) \le x \le Lp \end{cases} \qquad (55)$$

$$a > b: \qquad \tau(x) = \frac{m_2}{\lambda}Pb\left(1 - \frac{a}{L}\right)e^{-\lambda x} - m_1\frac{Pb}{L} \qquad 0 \le x \le Lp \qquad (56)$$

where P is the concentrated load (Fig. 3(b)) and $k = \lambda(b - a)$. The expression of m_1, m_2 and, takes into consideration the shear deformation of adherends.

Interfacial shear stress for two point loads
The general solution for the interfacial shear stress for this load (Fig. 3(c)) case is

$$a < b: \qquad \tau(x) = \begin{cases} \dfrac{m_2}{\lambda} Pae^{-\lambda x} + m_1 P - m_1 P\cosh(\lambda x)e^{-k} & 0 \le x \le (b\text{-}a) \\[3mm] \dfrac{m_2}{\lambda} Pae^{-\lambda x} + m_1 P\sinh(k)e^{-\lambda x} & (b\text{-}a) \le x \le \dfrac{Lp}{2} \end{cases} \qquad (57)$$

$$a > b: \qquad\qquad \tau(x) = \frac{m_2}{\lambda} Pbe^{-\lambda x} \qquad\qquad 0 \le x \le Lp \qquad (58)$$

Interfacial normal stress: general expression for all three load cases
The constants C_1 and C_2 are determined using the appropriate boundary conditions and they are written as follow

$$C_1 = \frac{K_n}{2\beta^3 E_1 I_1}\left[V_T(0) + \beta M_T(0)\right] - \frac{n_3}{2\beta^3}\tau(0) + \frac{n_1}{2\beta^3}\left(\frac{d^4\tau(0)}{dx^4} + \beta\frac{d^3\tau(0)}{dx^3}\right) \qquad (59)$$

$$C_2 = -\frac{K_n}{2\beta^2 E_1 I_1} M_T(0) - \frac{n_1}{2\beta^2}\frac{d^3\tau(0)}{dx^3} \qquad (60)$$

$$n_3 = b_2 K_n\left(\frac{e}{E_1 I_1} - \frac{D_{11}'t_2}{2b_2}\right) \qquad (61)$$

The above expressions for the constants C_1 and C_2 have been left in terms of the bending moment $M_T(0)$ and shear force $V_T(0)$ at the end of the soffit plate. With the constants C_1 and C_2 determined, the interfacial normal stress can then be found using Eq. (44) for all three load cases.

3. Comparison with experimental results

To validate the present method, a rectangular section is used here. One of the tested beams bonded with steel plate by Jones (Jones *et al.* 1988), beams F31, is analysed here using the present improved solution. The beam is simply supported and subjected to four-point bending, each at the third point. The geometry and materials properties of the specimen are summarized in the Table 1. The interfacial shear stress distributions in the beam bonded with a soffit steel plate under the applied load 60 kN , i.e., $P = 30$ kN , are compared between the experimental results and those obtained by the present method. As it can be seen from Fig. 4, the predicted theoretical results are in reasonable agreement with the experimental results.

Table 1 Dimensions and material properties

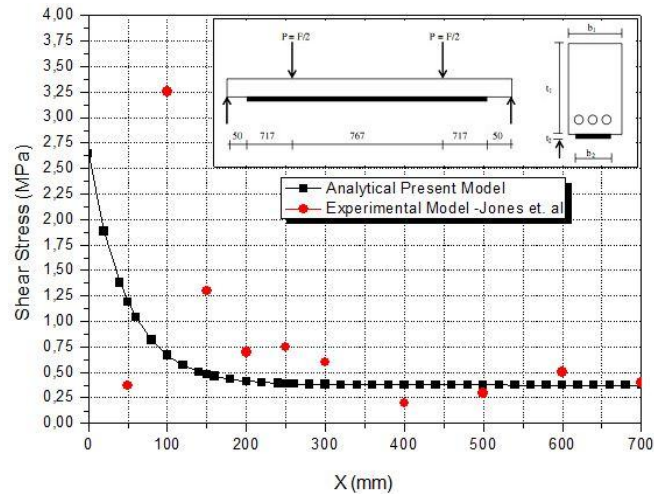|				
Concrete	$b_1 = 155$ mm	$t_1 = 255$ mm	$E_1 = 31$ MPa	
Steel	$b_2 = 125$ mm	$t_1 = 6$ mm	$E_2 = 200\,000$ MPa	
Adhesive	$b_a = b_2 = 125$ mm	$t_a = 1,5$ mm	$E_a = 280$ MPa	$G_a = 108$ MPa

Fig. 4 Comparison of interfacial shear of the steel plated RC beam with the experimental results

4. Results and discussion

Three cases are numerically studied. The first example focuses on the comparison between the interfacial stresses from the different existing methods and the present solution. In this example, the creep and shrinkage effect is not taken into account. In the second example, the time dependent behaviour of interface composite/RC beam is investigated. Finally, a parametric study is presented to show the effect of various parameters on the distributions of the interfacial stresses in an RC beam bonded with an FRP plate.

4.1 Material used

The material used for the present studies is an RC beam bonded with a glass or carbon fibre reinforced plastic (CFRP or GFRP) or with a steel plate. The beams are simply supported and subjected to a uniformly distributed load. A summary of the geometric and material properties is given in Table 2.

4.2 Comparison of analytical solutions

A comparison between the interfacial shear and normal stresses from the different existing

Table 2 Geometric and material properties

Material	E_{11} (GPa)	E_{22} (GPa)	G_{12} (GPa)	v_{12}	Width (mm)	Depth (mm)
CFRP plate	140	10	5	0.28	$b_f = 200$	$t_f = 4$
GFRP plate	50	10	5	0.28	$b_f = 200$	$t_f = 4$
Steel plate	200			0.3	$b_f = 200$	$t_f = 4$
RC beam	30	30		0.18	$b_f = 200$	$t_b = 300$
Adhesive layer	3	3		0.35	$b_f = 200$	$t_a = 4$

Table 3 Comparison of peak interfacial shear and normal stresses (MPa)

Load	Theory	RC beam with CFRP plate		RC beam with GFRP plate	
		τ	σ	τ	σ
UDL uniformly distributed load	Present	1.874	0.996	1.153	0.780
	Tounsi *et al*. 2009	1.791	1.078	1.085	0.826
	Smith and Teng 2001	3.834	2.101	1.975	1.244
mid-point load	Present	2.362	1.242	1.434	0.963
	Tounsi *et al*. 2009	2.051	1.234	1.228	0.935
	Smith and Teng 2001	4.310	2.364	2.677	1.837
two point loads	Present	2.045	1.223	1.276	0.939
	Tounsi *et al*. 2009	2.936	2.423	1.789	1.135
	Smith and Teng 2001	8.993	4.902	5.708	3.895

closed-form solutions, and the present new solution is undertaken in this section without taking the creep and shrinkage effect into account. An RC beam bonded with a CFRP soffit plate is being considered.

The beam is simply supported and subjected to a uniformly distributed load. A summary of the geometric and material properties is given in Table 2. The span of The RC beam is 3000 mm, the distance from the support to the end of the plate is 300 mm and the uniformly distributed load is 50 kN/m. Fig. 5 shows the distribution of the interfacial shear stress and the longitudinal normal stress near the plate end for the example RC beam bonded with a CFRP plate for the uniformly distributed load case. It can be seen from the figure that the stress distributions predicted by the present method are in good agreement with those obtained by using other methods.

The results of the peak interfacial shear and normal stresses (at the end of the soffit plate) are given in Table 3 for the RC beam strengthened by bonding GFRP and CFRP plate. As it can be
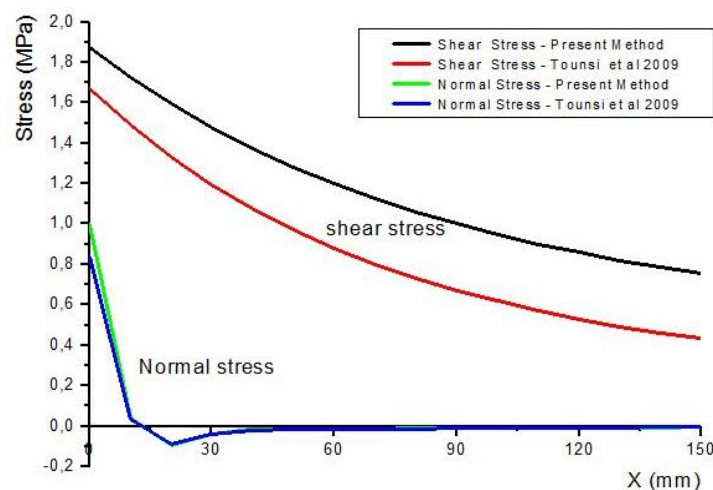

Fig. 5 Comparison of interfacial shear and normal stresses for an RC beam with a bonded CFRP soffit plate subjected to a uniformly distributed load (without creep and shrinkage effect)
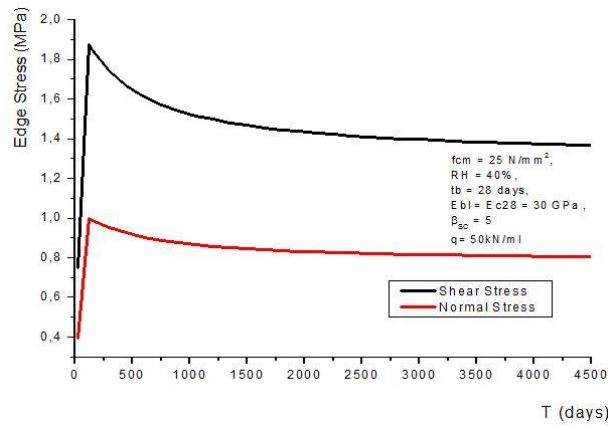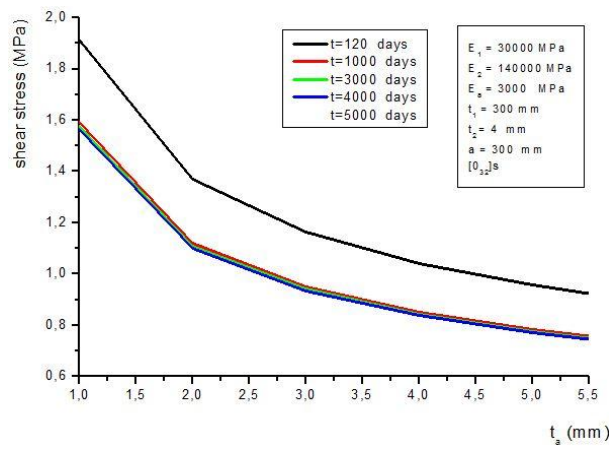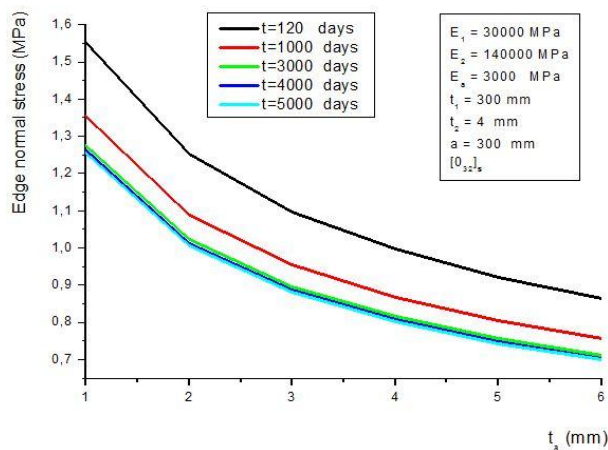
Fig. 6 Time development of interfacial edge stresses for an RC beam with a bonded CFRP soffit plate

(a)

(b)

Fig. 7 (a) Effect of adhesive layer thickness on edge shear stresses in CFRP strengthened RC beam;
(b) Effect of adhesive layer thickness on edge normal stresses in CFRP strengthened RC beam

seen from the results, the peak interfacial stresses assessed by the present theory are smaller compared to those given by Smith and Teng solution (2001). This implies that adherend shear deformation is an important factor influencing the adhesive interfacial stresses distribution.

4.3 Parametric study

In this section, numerical results of the present solutions are presented to study the effect of various parameters on the distributions of the interfacial stresses in an RC beam bonded with an FRP plate. These results are intended to demonstrate the main characteristics of interfacial stress distributions in these strengthened beams.

4.3.1 Effect of creep and shrinkage on edge interfacial stresses
On the basis of the presented analytical method, a computer program has been written and
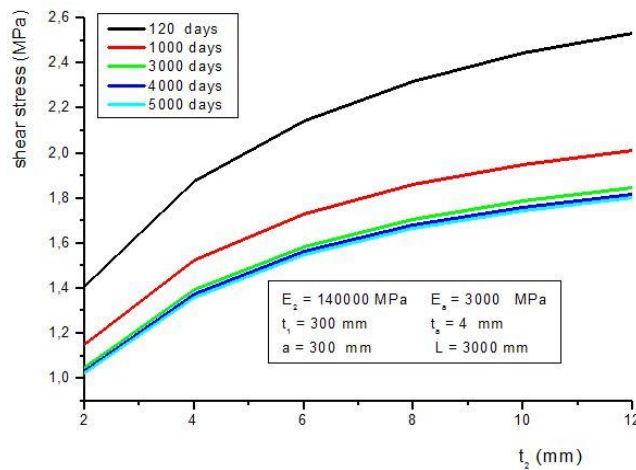
(a)
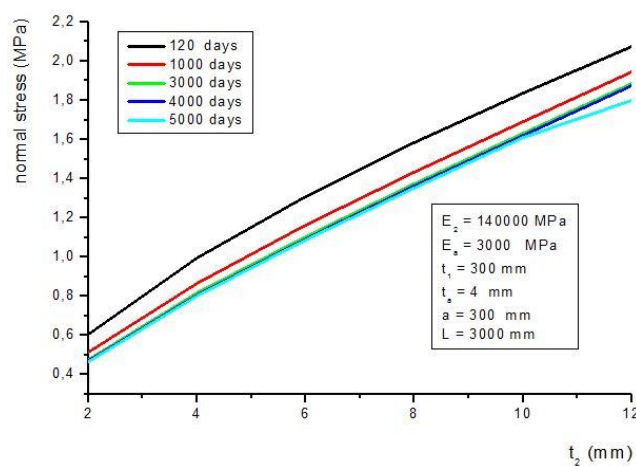
(b)

Fig. 8 (a) Effect of maximum edge shear stress with different thickness of CFRP;
(b) Effect of maximum edge normal stress with different thickness of CFRP

a representative example has been studied to demonstrate the effect of creep and shrinkage on edge interfacial stresses. In Fig. 6, the time development of the edge interfacial stresses is presented. From the obtained results we can conclude that the edge interfacial stresses exhibit the lower value after 28 days. These stresses take a peak value during the first months and begin to decrease until they become almost constant after a very long time.

4.3.2 Effect of adhesive layer thickness

Figs. 7(a) and (b) show the effects of the thickness of the adhesive layer on the interfacial stresses. Increasing the thickness of the adhesive layer leads to a significant reduction in the peak interfacial stresses. Thus using thick adhesive layer, especially in the vicinity of the edge, is recommended. In addition, it can be shown that these stresses decrease during time, until they become almost constant after a very long time.
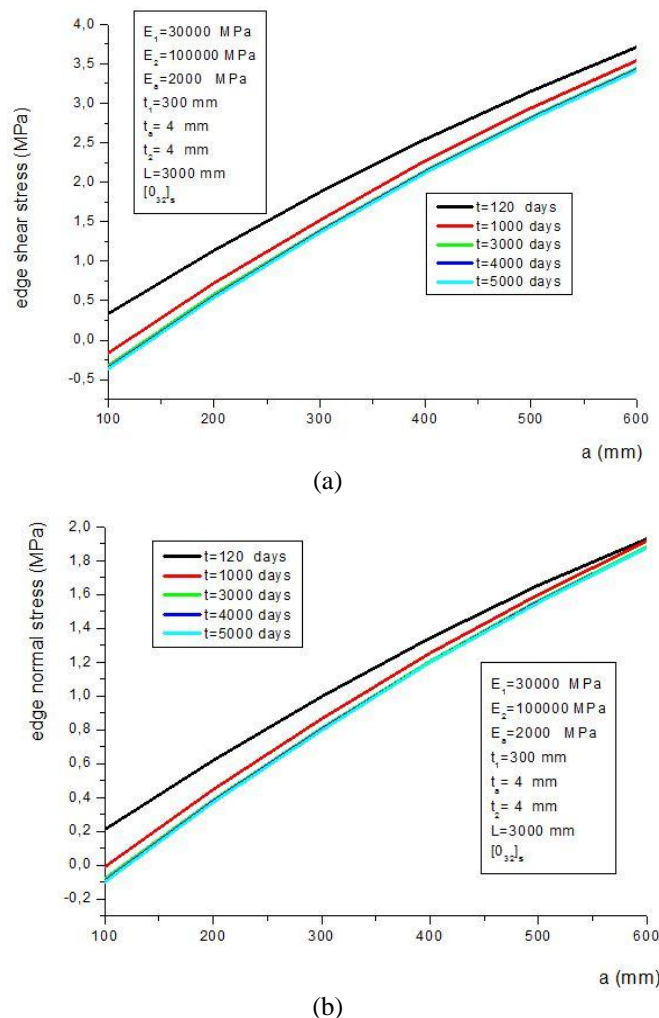

(a)

(b)

Fig. 9 (a) Influence of length of unstrengthened region on edge shear stress in CFRP strengthened RC beam; (b) Influence of length of unstrengthened region on edge normal stress in CFRP strengthened RC beam
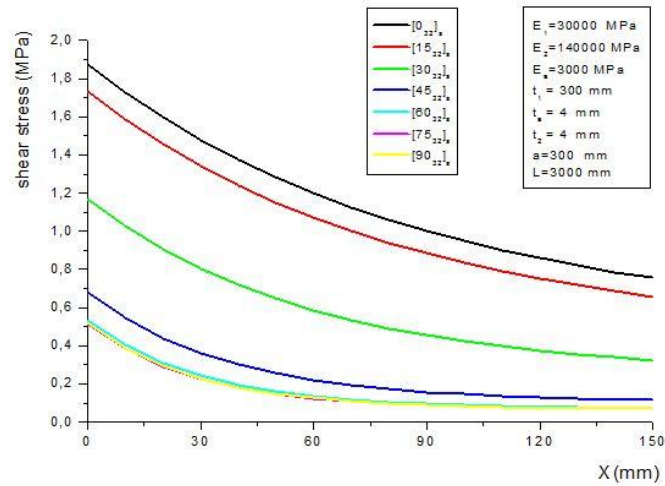
Fig. 10 Effect of the fiber orientation on the interfacial shear stresses for RC beam with a bonded CFRP soffit plate
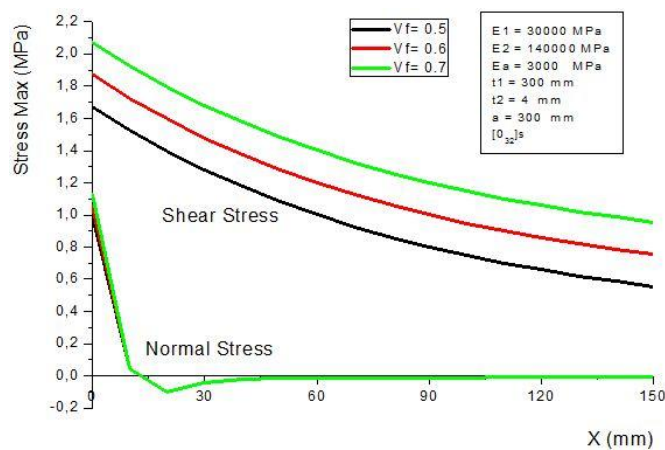

Fig. 11 The effect of fiber volume fraction on the variation of both shear and normal adhesive stresses in RC beam bonded with composite plate

4.3.6 Fiber volume fractions effect

Fig. 11 shows, the effect of fiber volume fractions V_f (= 0.5, 0.6 and 0.7) on the variation of shear and normal adhesive stresses. It can be seen that the interfacial shear stresses are reduced with decreases in fiber volume fraction. However, almost no effect is observed on the variation of interfacial normal stresses.

5. Conclusions

A simple closed-form solution to calculate the interfacial shear and normal stresses of retrofitted concrete beam strengthened with thin composite plate under mechanical loads including the creep and shrinkage effect has been presented in this paper. The evaluation of interfacial

stresses provides the basis for understanding plate-end debonding failures in such beam and for the development of suitable design rules. By comparing with experimental and analytical results, this solution provides satisfactory predictions to the interfacial stress in the plated beams, which demonstrates that the adherend shear deformations and the bending deformations in CFRP plate have only a very small effect. In the final part of this paper, extensive parametric studies were undertaken by using the new solution for strengthened beams with various ratios of design parameters.

The following conclusions to be drawn from this investigation are:

(1) The proposed solution permits the study of the behavior of composite plate –RC hybrid beams due to the opposed effects of creep and shrinkage.

(2) The maximum edge interfacial stresses increase with increasing alignment of all high strength fibers in CFRP plantain beam's longitudinal direction.

(3) The maximum edge interfacial stresses decrease as the thickness of the adhesive increases, the thickness of FRP plate decreases or the length of unstrengthened region decreases.

(4) The interfacial shear stresses are reduced with decreases in fiber volume fraction. However, almost no effect is observed on the variation of interfacial normal stresses.

(5) No effect on the variation of adhesive stresses is observed when we use hygrothermal aged FRP plate to strengthen the RC beam.

In conclusion, we can say that in addition to matrix composite fiber materials, another alternative may be proposed for strengthening structures, this will involve the use of functionally graded materials FGM (Bourada *et al*. 2015, Bennoun *et al*. 2016, Belabed *et al*. 2014, Bellifa *et al*. 2017, Bouafia *et al*. 2017, Bousahla *et al*. 2014, Abualnou *et al*. 2018 and Abdelaziz *et al*. 2017) in order to ensure continuity properties lift through the thickness of the reinforcement plate.

Acknowledgments

References

Abdelaziz, H.H., Meziane, M.A.A., Bousahla, A.A., Tounsi, A., Mahmoud, S.R. and Alwabli, A.S. (2017), "An efficient hyperbolic shear deformation theory for bending, buckling and free vibration of FGM sandwich plates with various boundary conditions", *Steel Compos. Struct*., *Int*. *J*., **25**(6), 693-704.

Abdelhak, Z., Hadji, L., Hassaine Daouadji, T. and Adda, B. (2016), "Thermal buckling response of functionally graded sandwich plates with clamped boundary conditions", *Smart Struct. Syst*., *Int*. *J*., **18**(2), 267-291.

Abualnour, M., Houari, M.S.A., Tounsi, A., Adda Bedia, E.A. and Mahmoud, S.R. (2018), "A novel quasi-3D trigonometric plate theory for free vibration analysis of advanced composite plates", *Compos. Struct*., **184**, 688-697.

Adim, B., Hassaine Daouadji, T., and Rabahi, A. (2016a), "A simple higher order shear deformation theory

for mechanical behavior of laminated composite plates", *Int. J. Adv. Struct. Eng.*, **8**(2), 103-117.

Adim, B., Hassaine Daouadji, T., Abbes, B. and Rabahi, A. (2016b), "Buckling and free vibration analysis of laminated composite plates using an efficient and simple higher order shear deformation theory", *J. Mech. Ind.*, **17**(5), p. 512.

Amara, K.H., Tounsi, A. and Benzair, A. (2005), "Transverse cracking and elastic properties reduction in hygrothermal aged crossply laminates", *Mater. Sci. Eng. A*, **396**(1-2), 369-375.

Ameur, M., Tounsi, A., Benyoucef, S., Bouiadjra, M.B. and Bedia, E.A. (2009), "Stress analysis of steel beams strengthened with a bonded hygrothermal aged composite plate", *Int. J. Mech. Mater.*, **5**(2), 143-156.

Belabed, Z., Houari, M.S.A., Tounsi, A., Mahmoud, S.R. and Bég, O.A. (2014), "An efficient and simple higher order shear and normal deformation theory for functionally graded material (FGM) plates", *Compos. Part B*, **60**, 274-283.

Bellifa, H., Bakora, A., Tounsi, A., Bousahla, A.A. and Mahmoud, S.R. (2017), "An efficient and simple four variable refined plate theory for buckling analysis of functionally graded plates", *Steel Compos. Struct., Int. J.*, **25**(3), 257-270.

Benferhat, R., Hassaine Daouadji, T., and Mansour, M.S. (2016), "Free vibration analysis of FG plates resting on the elastic foundation and based on the neutral surface concept using higher order shear deformation theory", *Comptes Rendus Mécanique*, **344**(9), 631-641.

Bennoun, M., Houari, M.S.A. and Tounsi, A. (2016), "A novel five variable refined plate theory for vibration analysis of functionally graded sandwich plates", *Mech. Adv. Mater. Struct.*, **23**(4), 423-431.

Benyoucef, S., Tounsi, A., Yeghnem, R., Bouiadjra, M.B. and Bedia, E.A. (2014), "An analysis of interfacial stresses in steel beams bonded with a thin composite plate under thermomechanical loading", *Mech. Compos. Mater.*, **49**(6), 959-972.

Bouafia, K., Kaci, A., Houari, M.S.A., Benzair, A. and Tounsi, A. (2017), "A nonlocal quasi-3D theory for bending and free flexural vibration behaviors of functionally graded nanobeams", *Smart Struct. Syst., Int. J.*, **19**(2), 115-126.

Bouakaz, K., Hassaine Daouadji, T., Meftah, S.A., Ameur, M., Tounsi, A. and Bedia, E.A. (2014), "A numerical analysis of steel beams strengthened with composite materials", *Mech. Compos. Mater.*, **50**(4), 685-696.

Bourada, M., Kaci, A., Houari, M.S.A. and Tounsi, A. (2015), "A new simple shear and normal deformations theory for functionally graded beams", *Steel Compos. Struct., Int. J.*, **18**(2), 409-423.

Bousahla, A.A., Houari, M.S.A., Tounsi, A. and Adda Bedia, E.A. (2014), "A novel higher order shear and normal deformation theory based on neutral surface position for bending analysis of advanced composite plates", *Int. J. Comput. Meth.*, **11**(6), 1350082.

Hassaine Daouadji, T. (2013), "Analytical analysis of the interfacial stress in damaged reinforced concrete beams strengthened by bonded composite plates", *Strength Mater.*, **45**(5), 587-597.

Hassaine Daouadji, T., Benyoucef, S., Tounsi, A., Benrahou, K.H. and Bedia, A.E. (2008), "Interfacial stress concentrations in FRP-damaged RC hybrid beams", *Compos. Interf.*, **15**(4), 425-440.

Hassaine Daouadji, T., Henni, A.H., Tounsi, A. and El Abbes, A.B. (2013), "Elasticity solution of a cantilever functionally graded beam", *Appl. Compos. Mater.*, **20**(1), 1-15.

Hassaine Daouadji, T., Benferhat, R. and Adim, B. (2016a), "A novel higher order shear deformation theory based on the neutral surface concept of FGM plate under transverse load", *Adv. Mater. Res.*, **5**(2), 107-123.

Hassaine Daouadji, T., Hadji, L., Meziane, M.A.A. and Bekki, H. (2016b), "Elastic analysis effect of adhesive layer characteristics in steel beam strengthened with a fiber-reinforced polymer plates", *Struct. Eng. Mech., Int. J.*, **59**(1), 83-100.

Hassaine Daouadji, T., Rabahi, A., Abbes, B. and Adim, B. (2016c), "Theoretical and finite element studies of interfacial stresses in reinforced concrete beams strengthened by externally FRP laminates plate", *J. Adhes. Sci. Technol.*, **30**(12), 1253-1280.

Draiche, K., Tounsi, A. and Mahmoud, S.R. (2016), "A refined theory with stretching effect for the flexure analysis of laminated composite plates", *Geomech. Eng., Int. J.*, **11**(5), 671-690.

Eurocode 2 Editorial Group (1991), Design of concrete structures, part 1: general rules and rules for buildings; Eurocode No. 2, Brussels.

Guenaneche, B. and Tounsi, A. (2014), "Effect of shear deformation on interfacial stress analysis in plated beams under arbitrary loading", *Int. J. Adhes. Adhes.*, **48**, 1-13.

Hamidi, A., Houari, M.S.A., Mahmoud, S.R. and Tounsi, A. (2015), "A sinusoidal plate theory with 5-unknowns and stretching effect for thermomechanical bending of functionally graded sandwich plates", *Steel Compos. Struct., Int. J.*, **18**(1), 235-253.

Hebali, H., Tounsi, A., Houari, M.S.A., Bessaim, A. and Bedia, E.A.A. (2014), "New quasi-3D hyperbolic shear deformation theory for the static and free vibration analysis of functionally graded plates", *ASCE J. Engineering Mechanics*, **140**(2), 374-83.

Jones, R., Swamy, R.N. and Charif, A. (1988), "Plate separation and anchorage of reinforced concrete beams strengthened by epoxy-bonded steel plates", *Struct. Eng.*, **66**(5), 85-94.

Krour, B., Bernard, F. and Tounsi, A. (2013), "Fibers orientation optimization for concrete beam strengthened with a CFRP bonded plate: A coupled analytical-numerical investigation", *Eng. Struct.*, **56**, 218-227.

Mahi, B.E., Benrahou, K.H., Belakhdar, K., Tounsi, A. and Bedia, E.A. (2014), "Effect of the tapered end of a FRP plate on the interfacial stresses in a strengthened beam used in civil engineering applications" , *Mech. Compos. Mater.* , **50**(4), 465-474.

Meier, U. (1995), "Strengthening of structures using carbon fibre/epoxy composites", *Constr. Build. Mater.*, **9**(6), 341-351.

Meziane, M.A.A., Abdelaziz, H.H. and Tounsi, A. (2014), "An efficient and simple refined theory for buckling and free vibration of exponentially graded sandwich plates under various boundary conditions", *J. Sandw. Struct. Mater.*, **16**(3), 293-318.

Rabahi, A., Adim, B., Chargui, S. and Hassaine Daouadji, T. (2015a), "Interfacial stresses in FRP-plated RC beams: effect of adherend shear deformations", In: *Multiphysics Modelling and Simulation for Systems Design and Monitoring*, Volume 2, pp. 317-326.

Rabahi, A., Hassaine Daouadji, T., Abbes, B. and Adim, B. (2015b), "Analytical and numerical solution of the interfacial stress in reinforced-concrete beams reinforced with bonded prestressed composite plate", *J. Reinf. Plastics Compos.*, **35**(3), 258-272.

Rabinovitch, O. and Frostig, Y. (2001), "Delamination failure of RC beams strengthened with FRP strips: a closed-form high order and fracture mechanics approach", *J. Eng. Mech. ASCE*, **127**(8), 852-861.

Roberts, T.M. and Hajikazemi, H. (1989), "A theoretical study of the behaviour of reinforced concrete beams strengthened by externally bonded steel plates", *Proceedings of the Institution of Civil Engineers*, **87**(1), 39-55.

Shen, H.S., Teng, J.G. and Yang, J. (2001), "Interfacial stresses in beams and slabs bonded with a thin plate", *J. Eng. Mech. ASCE*, **127**(4), 399-406.

Smith, S.T. and Teng, J.G. (2001), "Interfacial stresses in plated RC beams", *Eng. Struct.*, **23**(7), 57-71.

Täljsten, B. (1997), "Strengthening of beams by plate bonding", *J. Mater. Civil Eng. ASCE*, **9**(4), 6-12.

Touati, M., Tounsi, A. and Benguediab, M. (2015), "Effect of shear deformation on adhesive stresses in plated concrete beams: Analytical solutions", *Comput. Concrete, Int. J.*, **15**(3), 141-166.

Tounsi, A. (2006), "Improved theoretical solution for interfacial stresses in concrete beams strengthened with FRP plate", *Int. J. Solid Struct.*, 43, 54-74.

Tounsi, A., Hassaine Daouadji, T. and Benyoucef, S. (2009), "Interfacial stresses in FRP-plated RC beams: Effect of adherend shear deformations", *Int. J. Adhes. Adhes.*, **29**(4), 343-351.

Vilnay, O. (1988), "The analysis of reinforced concrete beams strengthened by epoxy bonded steel plates", *Int. J. Cement Compos. Lightweight Concrete*, **10**(2), 73-88.

Yang, J., Teng, J.G. and Chen, J.F. (2003), "A high-order closed-form solution for interfacial stresses in soffit plated RC beams under arbitrary loads", *Proceedings of the Institution of Civil Engineers – Struct. Build.*, **157,** 1-13.

Zidani, M.H.B., Belakhdar, K. and Tounsi, A. (2015), "Finite element analysis of initially damaged beams repaired with FRP plates", *Compos. Struct.*, **134**, 429-439.

Zidi, M., Tounsi, A., Houari, M.S.A. and Bég, O.A. (2014), "Bending analysis of FGM plates under hygro-thermo-mechanical loading using a four variable refined plate theory", *Aerosp. Sci. Technol.*, **34**, 24-34.

CC